Systems & Control Transactions

Original Research Article
Peer Reviewed Conference Proceeding
ESCAPE 36 - European Symposium on Computer Aided Process Engineering
Sheffield, UK. 21-24 June 2026

PSE PRESS

Techno-economic feasibility of gallium recovery from semiconductor wastewater

Kilian Kozerke[ab]*, Thomas Eberius[b], Nathanial J. Cooper[a]

[a] University of Cambridge, Department of Engineering, Cambridge, UK
[b] RWTH Aachen University, Faculty of Mechanical Engineering, Aachen, Germany
* Corresponding Author: kilian.kozerke@rwth-aachen.de, kozerke.work@gmail.com

ABSTRACT

Gallium is a critical material with increasing demand driven by compound semiconductors such as gallium nitride (GaN) and gallium arsenide (GaAs) used in power electronics and optoelectronics and a highly concentrated supply chain, with 98 % of refined production occurring in China. While recycling remains limited, GaAs semiconductor manufacturing generates wastewater that can contain gallium concentrations ranging from 1–35 mg·L^{-1}, representing an underutilized secondary resource. This study evaluates the technical and economic feasibility of recovering gallium from GaAs semiconductor wastewater across an input range of 10–100 m^3·d^{-1} using process modelling and a techno-economic analysis comparing two alternative separation routes: ion exchange (IX) and solvent extraction (SX). Using a real-world industrial wastewater composition, IX achieves a higher overall recovery than single-stage SX (80.40 % vs. 62.54 %), which translates into consistently lower levelized costs of gallium. The resulting levelized cost decreases from 563 to 144 €·kg^{-1} for IX and from 701 to 161 €·kg^{-1} for SX. The results demonstrate that separation step efficiency is the dominant determinant of economic performance and show that gallium recovery from semiconductor wastewater can be economically viable at fab-relevant scale. The analysis provides a proof-of-concept for integrating gallium recovery into semiconductor wastewater management and highlights its potential contribution to resource security and circular material supply.

Keywords: Gallium recovery, GaAs semiconductor wastewater, techno-economic analysis, ion exchange, solvent extraction, critical raw material, circular economy

INTRODUCTION

The compound semiconductor industry is a key enabler of renewable energy and low-carbon technologies through materials such as gallium arsenide (GaAs) and gallium nitride (GaN), which enable high-efficiency power electronics and optoelectronic devices [1]. Semiconductor applications include photovoltaics, power conversion in wind and solar technologies and the electrification of transport [1].

As demand increases, gallium has become a critical material with highly concentrated supply chains, as 98% of refined production occurs in China [2]. As a companion metal primarily derived from bauxite processing and aluminum refining, independent scale-up is challenging. Global demand is projected to exceed 3000 t by 2050 [3], yet total potential capacity in 2024 was only 1100 t and primary production output was around 760 t.

Recent export restrictions have exposed the fragility of this dependency, with gallium prices rising from below 185 € kg^{-1} in 2020 to more than 460 € kg^{-1} in 2023 [4]. These developments highlight the urgency of developing alternative and secondary gallium sources to enhance supply resilience and reduce exposure to geopolitical and regulatory disruptions.

Recycling of gallium remains negligible and is largely confined to production scrap, while end-of-life recovery is virtually absent [1]. Industrial wastewater from semiconductor manufacturing represents a promising yet underexplored secondary source of gallium. In particular, GaAs wastewater from wafer manufacturing has shown gallium concentrations of up to 35 mg L^{-1} [5]. Recent material flow analyses indicate that dominant gallium losses in both wafer- and device-oriented compound semiconductor manufacturing arise from the same unit

operations, particularly substrate processing and back-grinding, implying comparable gallium-bearing wastewater streams across these sectors [6]. A material flow analysis identified wafer and device production as major loss hotspots, accounting for 19 ± 5 % and 26 ± 5 % of gallium losses within the production system, respectively, and highlights wastewater treatment as a key leverage point for reducing these losses, revealing a substantial untapped recovery potential of both economic and environmental relevance [7].

To address this gap, this study compares two separation technologies: ion exchange (IX, e.g., chelating resins) and solvent extraction (SX, e.g., organophosphorus extractants). IX is the current state-of-the-art method and is already applied on a large industrial scale to recover gallium from Bayer® liquor, an alkaline process stream generated during alumina production, owing to its high selectivity and operational stability [8]. However, while IX dominates industrial gallium recovery from alkaline process streams, solvent extraction remains chemically well suited for acidic, arsenic-bearing solutions and is frequently reported in the literature on GaAs-related aqueous process solutions. For such systems, including scrap-derived leachates and simulated process solutions representative of GaAs manufacturing, both IX and SX have been tested mainly at laboratory scale, achieving high gallium recovery yields of up to 99 % and successful arsenic removal [9, 10].

Despite this demonstrated technical potential, neither technology has been implemented at scale for fab wastewaters, largely due to dilute gallium concentrations and complex co-contaminant matrices that undermine economic viability [5]. At the same time, recent laboratory studies report high selectivity and recovery for GaAs-representative acidic solutions, and emerging downstream conversion concepts offer additional enabling options; however, their implications for full-scale process design, cost drivers, and break-even conditions remain insufficiently quantified [9, 11, 12].

This work develops a system-level process model and techno-economic analysis to translate reported separation performance into scaled process designs and quantify cost drivers, break-even conditions, and design trade-offs across IX and SX. The results provide actionable design guidance for fab integration of resource recovery and water reuse and support policymakers and commodity strategists with quantitative evidence on circular supply options that can reduce dependence on highly concentrated primary gallium supply chains.

MATERIALS AND METHODS

Framework for the case study

This work develops and applies a techno-economic analysis (TEA) to evaluate the economic viability of gallium recovery from GaAs semiconductor wastewater. This section defines the case study, system boundaries, and modelling framework used to quantitatively compare two alternative recovery routes—ion exchange and solvent extraction.

First, process models, which include mass and energy balances to track gallium and key co-contaminants, are developed for each recovery train, identifying the major pretreatment, separation, and conversion steps for the two alternative separation technologies considered. The process models calculate gallium production rates, energy and additive demands, equipment quantities and sizes, and material replacement requirements, which are subsequently used as inputs to the techno-economic analysis. Next, a system-level TEA model calculates the levelized cost of gallium (LCOGa).

Key technical and economic inputs (feed composition, operating setpoints, performance parameters, costs and lifetime assumptions) are summarized in Tables 1–2 and applied consistently across both routes to ensure comparability. The TEA reports LCOGa and its decomposition into capital, operating, replacement, and labour cost contributions.

The case study is defined using measured wastewater compositions reported for real GaAs wafer manufacturing effluents. All economic parameters (electricity price, labour cost, and industrial cost indices) are referenced to a German industrial context, reflecting a representative European semiconductor manufacturing location. Gallium and arsenic concentrations of 34.6 mg L^{-1} and 35.3 mg L^{-1}, respectively, together with an acidic pH of 3.8, were taken from semiconductor wastewater characterized by Jain et al. and are used to define the representative feed composition in this work [5].

The wastewater is assumed to be available at continuous flow rates typical for industrial semiconductor fabrication facilities, reflecting segregated process wastewaters from shared unit operations such as back-grinding and etching that occur across both wafer and device manufacturing [6]. A throughput range of 10–100 m^3 d^{-1} was selected based on reported industrial effluent volumes and is applied consistently for equipment sizing, and cost correlations [13]. Additional aggregate water quality parameters, including total dissolved solids (TDS) and total suspended solids (TSS), were adopted from GaAs semiconductor wastewater treatment studies reported by Li et al. [14]. While Table 1 reports the key parameters used to define the case study, the process modelling accounts for the full wastewater composition reported in the literature.

As previously noted, this study examines IX and SX as the two alternative separation technologies for gallium recovery from GaAs semiconductor wastewater. In this work, the IX route is modelled using a chelating ion exchange resin (Diaion CR11) [12], while the SX route

employs an organophosphorus extractant (Cyanex 272) diluted in kerosene [9], consistent with experimental studies on gallium recovery from acidic GaAs-derived process solutions.

Table 1: Key feed characteristics and operating conditions defining the GaAs semiconductor wastewater case study

Parameter	Unit	Value	Source
Volume flow	$m^3\ d^{-1}$	10–100	[13]
Temperature	°C	25	[13]
pH		3.8	[5]
Gallium	$mg\ L^{-1}$	34.6	[5]
Arsenic	$mg\ L^{-1}$	35.3	[5]
Total dissolved solids	$mg\ L^{-1}$	1500	[14]
Total suspended solids	$mg\ L^{-1}$	30	[14]

These two separation technologies are evaluated as alternative recovery routes under identical wastewater feed definitions and system boundaries, enabling a consistent techno-economic comparison. The selected wastewater dataset therefore serves as a well-documented blueprint case for system-level modelling of gallium recovery from semiconductor wastewater.

This study targets the recovery of gallium with a purity of 99.99 % (4N). This grade is the standard commercial form of commodity gallium and is subsequently refined to high-purity (6N to 7N) for semiconductor device fabrication. Using this framework, the levelized cost of 4N gallium production is compared against current market prices, which were approximately 423 € kg^{-1} in 2024 [4].

Techno-economic analysis

The objective function to be minimized is the LCOGa, defined as the total annual cost of the system TC divided by the total annual production of 4N gallium, $m_{\mathrm{Ga,ann}}$ ($kg{\cdot}a^{-1}$):

$$LCOGa = \frac{TC}{m_{Ga,ann}} \tag{1}$$

The total annual gallium production is a function of the wastewater feed flow rate (Q_{feed}), the initial gallium concentration (c_{Ga}), the plant availability factor (y), and the overall recovery rate (TR), which is calculated from the process models developed in this work:

$$m_{Ga,ann} = Q_{feed} \times c_{Ga} \times TR \times y \times 365\ days \tag{2}$$

The total annualized cost of the gallium recovery system is defined as:

$$TC = AF \times CapEx + OpEx + Rep + LC \tag{3}$$

where $CapEx$ represents the capital expenditure required to install the gallium recovery process train, AF is the annualization factor, $OpEx$ denotes the annual operating expenses, Rep accounts for annualized replacement costs of materials and equipment with finite lifetimes, LC represents labour costs associated with plant operation.

The formula for the annualization factor is dependent on the annual discount rate, r, and the project lifetime in years, n:

$$AF = \frac{r(1+r)^n}{(1+r)^n - 1} \tag{4}$$

Capital expenditures are calculated by summing purchased equipment costs across all process steps and applying step-specific Lang factors $f_{Lang,s}$, to convert purchased costs to installed costs (accounting for installation, piping, instrumentation, for example):

$$CapEx = \sum_s (f_{Lang,s} \times \sum C_{equip,s}) \tag{5}$$

Here, $\sum C_{\mathrm{equip},s}$ is the total purchased cost of all equipment items assigned to process step s, and is the corresponding step-specific Lang factor.

Operating expenditures comprise electricity costs, chemical/additive consumption, and operations & maintenance (O&M) costs. Electricity costs are calculated from the annual electricity demand E_{ann} and the electricity price EP, while chemical costs depend on the annual consumption $m_{k,\,\mathrm{ann}}$ and unit price AP_k of each chemical or additive k. O&M costs are approximated as a fixed fraction OM of installed $CapEx$:

$$OpEx = E_{ann} \times EP + \sum_k (m_{k,ann} \times AP_k) + OM \times CapEx \tag{6}$$

Annual replacement costs Rep account for equipment and materials with finite lifetimes. They are calculated by annualizing the purchased cost of each replaceable item $C_{\mathrm{equip},i}$ over its expected lifetime τ_i:

$$Rep = \sum_i \frac{C_{equip,i}}{\tau_i} \tag{7}$$

The annual labour cost contribution, LC, is calculated as:

$$LC = C_{FTE} \times f_{FTE} \tag{8}$$

where C_{FTE} is the annual fully loaded cost of one full-time equivalent (FTE) employee, including salary, social charges, overhead, and benefits, and f_{FTE} is the fraction of a full-time equivalent required for operation of the gallium recovery process.

Values for the key parameters used in the analysis can be found in Table 2. It is worth noting that performance figures for the RO98pHt membrane, IX resin, SX, and electrowinning (EW) are sourced from experimental studies.

Table 2: Key parameters for the techno-economic analysis and the values associated with them.

Parameter symbol	Description	Value	Source
n	Plant lifetime	20	[15]
y	Availability factor	0.95	[15]
r	Discount factor	0.08	[16]
OM	Annual rate cost of operations and maintenance	0.02	[16]
EP	Electricity price [€ kWh^{-1}]	0.1648	[17]
C_{FTE}	Annual labour cost [€ a^{-1}]	69, 164	[18]
f_{FTE}	Fraction of an FTE	0.25	[19]
f_{Lang}	Lang factor	1.4 – 4.9	[20–22]
AP_{HCL}	Cost of hydrochloric acid feedstock [€ kg^{-1}]	0.15	[23]
AP_{H2SO4}	Cost of sulfuric acid feedstock [€ kg^{-1}]	0.13	[23]
AP_{NaOH}	Cost of sodium hydroxide feedstock [€ kg^{-1}]	0.3	[24]
C_{IX}	IX resin cost [€ kg^{-1}]	138.91	[25]
τ_{IX}	IX resin lifetime [y]	5	[26]
C_{SX}	SX extractant cost [€ kg^{-1}]	10	[27]
f_{makeup}	SX make up rate [% a^{-1}]	15	[28]
SEC_{EW}	EW energy [kWh kg^{-1} Ga]	9.05	[11]
$C_{RO98pHT}$	RO98pHt membrane cost [€ pc^{-1}]	1, 088	[29]

RESULTS AND DISCUSSION

Process trains and models

Process trains for each separation technology, IX and SX, were developed to recover 4N gallium from GaAs semiconductor wastewater. As shown schematically in Figure 1, both trains share an identical pretreatment and concentration front-end and a shared downstream conversion block; they differ only in the separation step. This structure enables a controlled comparison in which route-level differences in recovery and cost are dominated by separation performance and its implications for downstream conditioning.

The process begins with filtration to reduce suspended solids and mitigate downstream fouling while preserving dissolved species, including Ga [20]. Reverse osmosis (RO) is then used as a concentrator to reduce the flow volume and increase gallium concentration, improving the feasibility of selective recovery at comparatively small, fab-relevant module throughputs. The RO design uses a commercial spiral-wound membrane configuration (RO98pHt), which has demonstrated high rejection of multivalent ions and dissolved metals in acidic, metal-bearing waters [30]. In the process model, RO is implemented as a volumetric split with component-specific partitioning of gallium (and other tracked species) between permeate and concentrate. The permeate stream is treated as a reuse or discharge stream depending on site-specific integration, while the concentrate is routed to chemical conditioning [31].

The RO concentrate is adjusted to pH 2 using hydrochloric acid to ensure a stable operating window compatible with both separation routes and to avoid premature hydroxide precipitation. This setpoint follows reported operating conditions for gallium recovery in acidic solutions and provides a consistent basis for comparing IX and SX under the same feed chemistry. [9, 12, 23]

In the IX process train, Ga^{3+} is selectively complexed on a chelating resin and subsequently recovered through an acid wash. This step yields a gallium-rich product stream, while the treated aqueous stream leaving the column constitutes a gallium-depleted waste stream. Diaion CR-11 is used as the baseline resin and it is regenerated using 0.1 M H_2SO_4, consistent with reported gallium recovery from GaAs-derived feeds and supported by manufacturer specifications and literature data [12].

In the SX process train, gallium is transferred from the aqueous phase into an organic phase consisting of Cyanex 272 diluted in kerosene via pH-dependent complex formation, and subsequently stripped into an aqueous recovery solution using 0.5 M HCl, consistent with experimental studies on simulated GaAs waste etching solutions and hydrometallurgical practice [9]. Solvent make-up is explicitly included in the model to account for extractant losses and operability constraints relevant to industrial scale-up. The IX and SX recovery streams differ in acid chemistry (sulfate versus chloride), which propagates to downstream neutralization requirements and associated reagent demand.

After separation and regeneration, the gallium-rich recovery streams are not directly suitable for electrowinning due to their low gallium concentration, acidic chemistry, and residual matrix components, which would lead to severe hydrogen evolution and poor current efficiency. To enable efficient electroreduction, gallium is therefore first precipitated as gallium hydroxide by alkalinization using sodium hydroxide, effecting a solid–liquid separation that concentrates gallium while removing the bulk aqueous matrix and associated impurities [8].

The precipitate is then subjected to alkaline leaching to generate a gallium-rich electrolyte suitable for electroreduction [11]. This step is essential because direct

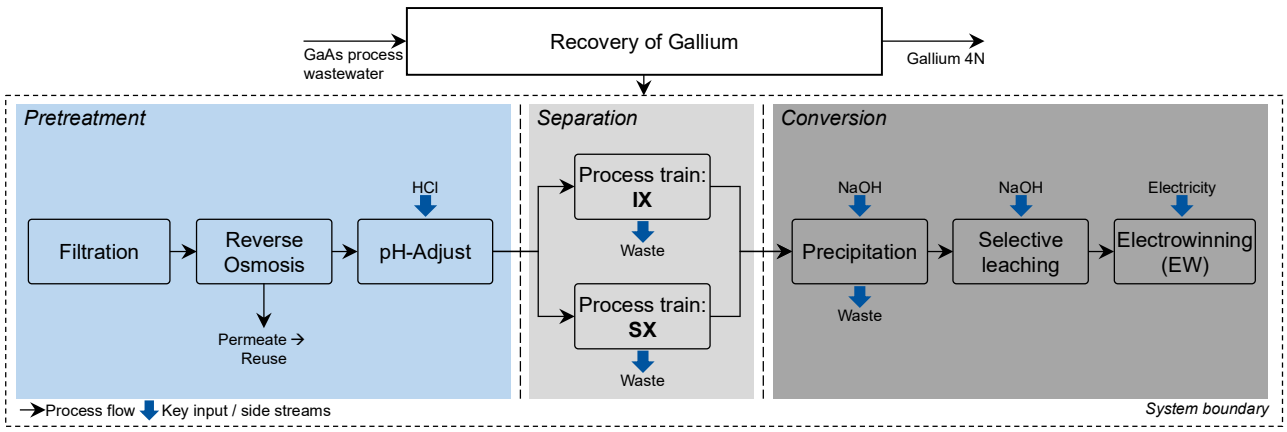

Figure 1: Schematic diagram of the processing trains developed and analyzed for recovery of 4N gallium from GaAs process wastewater, structured into pretreatment, separation, and conversion blocks. Pretreatment comprises filtration followed by reverse osmosis (RO), operated as a volumetric split to concentrate gallium in the retentate while generating a permeate stream assumed available for reuse. The RO concentrate is chemically conditioned by pH adjustment to establish an acidic matrix suitable for selective gallium separation.
Two alternative separation technologies are considered: (i) ion exchange (IX), in which gallium is selectively adsorbed on a chelating resin and recovered by acid elution; and (ii) solvent extraction (SX), in which gallium is transferred into an organic phase and subsequently stripped into an aqueous recovery stream. In both cases, the gallium-rich stream is routed to a shared conversion train comprising precipitation, alkaline leaching, and electrowinning to produce 4N gallium using a titanium cathode. The dashed box indicates the system boundary. Black arrows denote the main process flow, while blue arrows indicate key chemical and utility inputs as well as qualitative side streams.

electrowinning from acidic recovery solutions would be kinetically unfavorable and dominated by hydrogen evolution.

Final recovery is achieved by electrowinning using a titanium cathode, following the cyclone electrowinning concept reported by Xu et al [11]. In this process, forced electrolyte circulation enhances mass transfer and suppresses concentration polarization, enabling stable deposition of metallic gallium from alkaline solutions. The deposited metallic gallium is mechanically separated, washed, and vacuum-dried to remove residual electrolyte and moisture, yielding 4N gallium as the final product, which represents the standard commercial grade and serves as feedstock for subsequent high-purity upgrading. [11]

Table 3: The fraction of gallium recovered using each process train for both technologies.

Process train	Recovery fraction
IX	80.4 %
SX	62.54 %

Overall gallium recovery for each train is computed from the stepwise recovery fractions across RO, separation, precipitation, leaching, and electrowinning, with the corresponding recovery values reported in Table 3. Because both routes share the same front-end and downstream conversion, differences in overall recovery are dominated by separation performance: IX achieves a single-pass recovery of 96.9 %, whereas single-stage SX is limited to 77.3 %, resulting in overall recoveries of 80.40 % and 62.54 %, respectively. In the baseline, the SX route is modelled as a single extraction/stripping stage following Chen et al., such that higher recovery would require additional stages and increased solvent inventory, implying a cost–recovery trade-off [9]. In contrast, the IX basis follows Cheng et al. and provides higher effective single-pass recovery due to strong Ga^{3+} affinity and efficient elution, thereby reducing separation-stage losses [12].

Techno-economic performance

The process models assume an unpressurized feed, with all unit operations sized explicitly using flow-dependent design equations and operating setpoints. Given the comparatively small target throughputs considered in this study (baseline feed flow rates of 10–100 $m^3\ d^{-1}$), a bottom-up costing approach is adopted based on explicit equipment sizing and vendor or literature pricing [32]. Generic large-plant cost correlations are not applied, as they are sparse or non-representative at this scale [20].

Waste and side streams (e.g., spent regenerant, RO permeate, spent electrolyte) are quantified for mass-balance closure, disposal costs for these streams are not charged to the recovery system in the baseline TEA. This

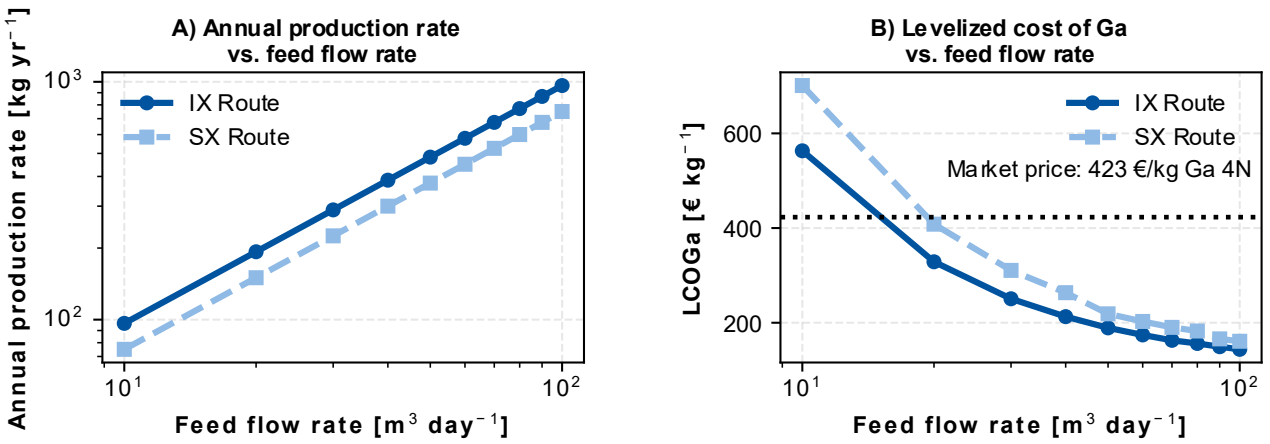

Figure 2: Baseline techno-economic results for gallium recovery from GaAs semiconductor wastewater comparing ion exchange (IX) and solvent extraction (SX) over feed flow rates of Q = 10–100 m^3 d^{-1}. (A) Annual production rate (kg yr^{-1}) versus feed flow rate (log–log), showing near-linear scaling with throughput at fixed feed composition and route-dependent yield differences arising from different overall recovery. (B) Levelized cost of gallium (€/kg 4N Ga) versus feed flow rate (log-x), including a reference market price for 4N gallium (423 €/kg).

framing represents an incremental "bolt-on" recovery module at a fab site with existing wastewater treatment infrastructure; stand-alone deployment would require explicit treatment/disposal costing and may shift the economic results [33].

The production rate shown in Figure 2A scales linearly with the feed flow rate. The factors determining annual production in these designs are primarily the total recovery and conversion yields across the process train (Table 3), which depend on separation performance (recovery and selectivity), reaction yields, and operational setpoints, rather than on the absolute volume of feed processed. Accordingly, the model applies fixed recovery fractions for each route in the baseline case, resulting in proportional scaling of annual production with Q. At the baseline composition (c_{Ga} = 34.6 mg L^{-1}), the IX route produces 96 kg per year at Q = 10 m^3 per day and 965 kg per year at Q = 100 m^3 per day, whereas the SX route produces 75 kg per year and 750 kg per year at the same throughputs. This difference in yield is not merely a production metric: because the LCOGa is normalized per kilogram of product, a lower total recovery reduces the denominator (kilograms of gallium produced per cubic meter processed) and therefore increases the cost in euros per kilogram, even if the processing cost per cubic meter were unchanged.

The levelized cost trends are shown in Figure 2B. LCOGa decreases steeply with throughput for both routes, falling from 563 to 144 € kg^{-1} for IX and from 701 to 161 € kg^{-1} for SX when scaling Q from 10 to 100 m^3 per day. The IX route is consistently lower in cost because it combines a higher overall recovery with a more favourable operating-cost structure at scale. This effect is particularly evident at Q = 100 m^3 d^{-1}, where operating expenses account for a larger fraction of total cost for SX, approximately 43%, compared to approximately 24% for IX, as shown in Figure 3. This is consistent with the additional consumables and operational burdens associated with the SX route in the baseline model.

To assess economic viability, the LCOGa curves are compared against a representative market price for 4N gallium of 423 € kg^{-1}. Both routes reach economic viability within the evaluated throughput range. Interpolation of the base-case LCOGa curves yields break-even throughput thresholds of approximately Q* = 14.2 m^3 d^{-1} for IX and Q* = 19.3 m^3 d^{-1} for SX under baseline assumptions. These thresholds provide a practical screening criterion for deployment: below Q* the recovery module is not viable at baseline performance, whereas above Q* it becomes viable without requiring optimistic price assumptions.

Figure 3 decomposes LCOGa into CapEx, OpEx, replacement, and labour to better understand the major cost drivers of the LCOGa. At Q = 10 $m^3 \cdot d^{-1}$, labour and annualized CapEx dominate for both routes (~30 % each), consistent with a small-plant regime where fixed and semi-fixed costs are spread over limited production. At Q = 100 $m^3 \cdot d^{-1}$, labour becomes less significant (~12–13 %), while CapEx and OpEx dominate, explaining the strong decline in €·kg^{-1} with scale.

In this bottom-up model, most variable consumptions (electricity, reagents, membrane area, and separation materials) scale approximately with treated volume, so returns to scale arise mainly from dilution of fixed/semi-fixed costs rather than improved specific consumptions. Parts of the installed equipment are also

discretely sized (e.g., standard pumps/ancillaries), such that selected items can cover a wide operating window and contribute similar installed costs at Q = 10 and 100 $m^3 \cdot d^{-1}$, producing stepwise CapEx behaviour. Consequently, within the two-train comparison, the most effective levers to reduce LCOGa are higher overall recovery TR (dominated by separation) and reductions in labour intensity and replacement burden.

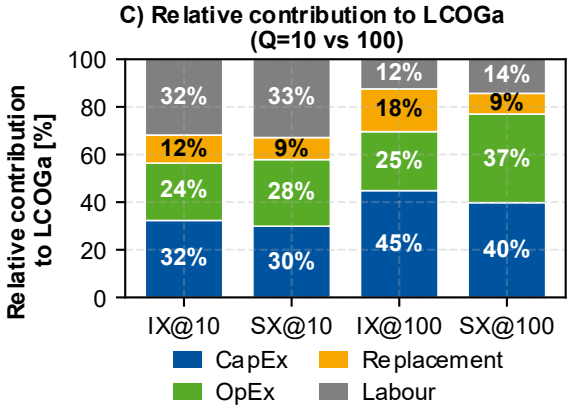

Figure 3: (C) Relative contribution of aggregated cost centres to the levelized cost of gallium (LCOGa) at two representative scales (Q = 10 and 100 $m^3\ d^{-1}$) for both routes

Deployment implications follow directly from the controlled IX vs. SX comparison. First, throughput and feed concentration jointly determine viability, as production scales with Q and c_{Ga} at fixed recovery (Eq. 2). Second, within the two-train comparison the dominant technical lever is overall recovery TR, driven primarily by the separation step; higher SX recovery would require additional stages and solvent inventory, introducing a clear cost–recovery trade-off. Third, the strong cost decline with scale indicates two regimes: at low feed flow rates, fixed and semi-fixed costs (labour, annualised equipment) dominate, whereas at higher feed flow rates consumables and energy become increasingly important.

CONCLUSION

This study assessed the techno-economic feasibility of recovering 4N gallium from GaAs semiconductor wastewater (c_{Ga} = 34.6 $mg \cdot L^{-1}$, pH = 3.8) across a throughput range of 10–100 $m^3 \cdot d^{-1}$. Under identical system boundaries with shared pretreatment and downstream conversion, ion exchange (IX) achieves higher overall recovery than single-stage solvent extraction (SX) (80.40 % vs. 62.54 %), resulting in consistently lower LCOGa across the evaluated range (144–563 $€ \cdot kg^{-1}$ for IX vs. 161–701 $€ \cdot kg^{-1}$ for SX). This performance gap is driven primarily by the markedly higher single-pass separation efficiency of IX (96.9% vs. 77.3% for SX), which dominates recovery losses and propagates directly into total plant recovery and cost. Compared against a representative 4N gallium market price of 423 $€ \cdot kg^{-1}$, the corresponding break-even throughputs are Q* ≈ 14.2 $m^3 \cdot d^{-1}$ for IX and 19.3 $m^3 \cdot d^{-1}$ for SX, providing a transferable proof-of-concept blueprint for bolt-on integration of gallium recovery into semiconductor fabrication facilities.

Future work should quantify environmental performance and investigate the cost–recovery trade-offs of multi-stage SX configurations to overcome single-stage limitations. In parallel, sensitivity analyses should be used to test the robustness and transferability of these findings across different wastewater flow rates, gallium concentrations, and semiconductor wastewater chemistries, and to explore their implications for wider deployment of gallium recovery across the semiconductor industry.

DIGITAL SUPPLEMENTARY MATERIAL

The Python code and input files required to reproduce the results of this study are available at: https://github.com/Kilian-Kozerke/escape36-gallium-tea

REFERENCES

1. Løvik AN, Restrepo E, Müller DB. The global anthropogenic gallium system: determinants of demand, supply and efficiency improvements. Environ. Sci. Technol. 49:5704-5712 (2015). https://doi.org/10.1021/acs.est.5b00320
2. Jaskula B Mineral commodity summaries 2024.
3. Song H, Wang C, Sen B, Liu G. China factor: exploring the byproduct and host metal dynamics for gallium–aluminum in a global green transition. Environ. Sci. Technol. 56:2699-2708 (2022). https://doi.org/10.1021/acs.est.1c04784
4. Jaskula B Mineral commodity summaries 2025.
5. Jain R, Fan S, Kaden P, Tsushima S, Foerstendorf H, Barthen R, Lehmann F, Pollmann K. Recovery of gallium from wafer fabrication industry wastewaters by desferrioxamine b and e using reversed-phase chromatography approach. Water Research 158:203-212 (2019). https://doi.org/10.1016/j.watres.2019.04.005
6. Han Z, Liu Q, Ouyang X, Song H, Gao T, Liu Y, Wen B, Dai T. Tracking two decades of global gallium stocks and flows: a dynamic material flow analysis. Resources, Conservation and Recycling 202:107391 (2024). https://doi.org/10.1016/j.resconrec.2023.107391
7. Ueberschaar M, Otto SJ, Rotter VS. Challenges for critical raw material recovery from WEEE – the case study of gallium. Waste Management 60:534-545

(2017). https://doi.org/10.1016/j.wasman.2016.12.035
8. Luo H, Huang TY, Wu X, Zhao F. Life cycle assessment for primary gallium production at industrial-scale. Int J Life Cycle Assess 30:1545-1559 (2025). https://doi.org/10.1007/s11367-025-02492-1
9. Chen WS, Tien KW, Wang LP, Lee CH, Chung YF. Recovery of gallium from simulated gaas waste etching solutions by solvent extraction. Sustainability 12:1765 (2020). https://doi.org/10.3390/su12051765
10. Nguyen TH, Lee MS. A review on separation of gallium and indium from leach liquors by solvent extraction and ion exchange. Mineral Processing and Extractive Metallurgy Review 40:278-291 (2018). https://doi.org/10.1080/08827508.2018.1538987
11. XU ZP, LIU ZW, GUO XY, LI D, ZOU MJ, TIAN QH. Gallium recovery by cyclone electrowinning from alkaline electrolyte with titanium cathode. Transactions of Nonferrous Metals Society of China 34:1027-1036 (2024). https://doi.org/10.1016/s1003-6326(23)66451-9
12. Cheng TH, Liu CJ, Tsai TY, Shen YH. A process for the recovery of gallium from gallium arsenide scrap. Processes 7:921 (2019). https://doi.org/10.3390/pr7120921
13. Huang C, Pan JR, Lee M, Yen S. Treatment of high?level arsenic?containing wastewater by fluidized bed crystallization process. J of Chemical Tech & Biotech 82:289-294 (2007). https://doi.org/10.1002/jctb.1671
14. Li A, Luo J, Xu W, Pan T. Arsenic removal of high-arsenic wastewater from gallium arsenide semiconductor production by enhanced two-stage treatment. Desalination and Water Treatment :1-8 (2014). https://doi.org/10.1080/19443994.2014.927795
15. Kettani M, Bandelier P. Techno-economic assessment of solar energy coupling with large-scale desalination plant: the case of morocco. Desalination 494:114627 (2020). https://doi.org/10.1016/j.desal.2020.114627
16. Helal AM, Al-Malek SA, Al-Katheeri ES. Economic feasibility of alternative designs of a PV-RO desalination unit for remote areas in the united arab emirates. Desalination 221:1-16 (2008). https://doi.org/10.1016/j.desal.2007.01.064
17. SMARD | industriestrompreise. SMARD | Industriestrompreise. [Accessed: 22 Jan. 2026] https://www.smard.de/page/home/topic-article/211972/215546/industriestrompreise.
18. Chemiewirtschaft in zahlen - 2024.
19. Pryce D, Kapelan Z, Memon FA. Economic evaluation of a small wastewater treatment plant under different design and operation scenarios by life cycle costing. Development Engineering 7:100103 (2022). https://doi.org/10.1016/j.deveng.2022.100103
20. Peters MS et al. Plant design and economics for chemical engineers. (2004).
21. Huang X, Guida S, Jefferson B, Soares A. Economic evaluation of ion-exchange processes for nutrient removal and recovery from municipal wastewater. npj Clean Water 3: (2020). https://doi.org/10.1038/s41545-020-0054-x
22. Malek A, Hawlader MNA, Ho JC. Design and economics of RO seawater desalination. Desalination 105:245-261 (1996). https://doi.org/10.1016/0011-9164(96)00081-1
23. Amusat OO, Dudchenko AV, Atia AA, Bartholomew T. Cost-optimal selection of ph control for mineral scaling prevention in high recovery reverse osmosis desalination. Systems and Control Transactions 3:253-260 (2024). https://doi.org/10.69997/sct.143335
24. Mike Sodium hydroxide price index.
25. Diaion™ cr11(na), chelating resin, highly porous type, 0.5 mmole/ml on poly(styrene-divinylbenzene) 1 kg. Diaion™ CR11(Na), chelating resin, highly porous type, 0.5 mmole/ml on poly(styrene-divinylbenzene) 1 kg. [Accessed: 22 Jan. 2026] https://www.thermofisher.com/order/catalog/product/046544.A1.
26. AldexChemical-resin-service-life-guide.
27. Buy cyanex 272(83411-71-6) from luyunjia chemistry xiamen limited. Buy Cyanex 272(83411-71-6) from LUYUNJIA CHEMISTRY XIAMEN LIMITED. [Accessed: 22 Jan. 2026] https://www.echemi.com/produce/pr2503031015-cyanex-27283411-71-6.html.
28. Kaminski MD and I (United S Argonne National Lab. Evaluation of extractant-coated magnetic microparticles for the recovery of hazardous metals from waste solution.
29. Membrane & hsn code 8421 exports from denmark. Membrane & HSN Code 8421 Exports from Denmark. [Accessed: 22 Jan. 2026] https://www.volza.com/p/membrane/export/export-from-denmark/hsn-code-8421/.
30. Ambiado K, Bustos C, Schwarz A, Bórquez R. Membrane technology applied to acid mine drainage from copper mining. Water Science and Technology 75:705-715 (2016). https://doi.org/10.2166/wst.2016.556
31. Mendret J, Azais A, Favier T, Brosillon S. Urban wastewater reuse using a coupling between nanofiltration and ozonation: techno-economic

assessment. Chemical Engineering Research and Design 145:19-28 (2019). https://doi.org/10.1016/j.cherd.2019.02.034
32. Mohajerani S, Kumar A, Oni AO. A techno-economic assessment of gas-to-liquid and coal-to-liquid plants through the development of scale factors. Energy 150:681-693 (2018). https://doi.org/10.1016/j.energy.2018.03.005
33. Hess JC Chip production's ecological footprint: mapping climate and environmental impact.